PRODUCTION PROCESS

Joining by laser shock forming: realization and acting pressures

Stefan Veenaas · Hanna Wielage · Frank Vollertsen

Abstract The need to implement more functionality on the same space drives miniaturization and makes hybrid joints under various conditions also in the micro range necessary. Existing solutions often have restrictions due to the principle of joining. Thus, in this article a new high speed joining method for the micro range is presented, which is realized by a plastic forming process based on TEA-CO_2-laser induced shockwaves. In a first step it is shown how sheet–sheet joints can be realized with this method. In order to get knowledge of basic process parameter and for further application of the process, the near-by-field of acting pressure of the initiated shock wave is measured in open and tube environment. The results show that constant maximum acting pressure conditions appear in a tube, while pressure characteristics show high reflection phenomena. Furthermore, it is determined that the ignition point of the TEA-CO_2-laser induced plasma out of aluminum is about 8 mm above the surface.

Keywords High speed forming · Laser shock forming · Shock wave · Shock wave pressure · Joining

S. Veenaas (✉) · H. Wielage · F. Vollertsen
Bremer Institut für angewandte Strahltechnik GmbH (BIAS),
Klagenfurter Str. 2, 28359 Bremen, Germany
e-mail: veenaas@bias.de

H. Wielage
e-mail: wielage@bias.de

F. Vollertsen
e-mail: vollertsen@bias.de

1 Introduction

The ongoing trend of miniaturization in manufacturing processes, i.e. in precision mechanics and electronic industry, requires the use of manufacturing and especially joining processes in smaller dimensions. This brings increased demands, i.e. in accuracy, on joining processes. Conventional joining processes, which are used in macro range, cannot be easily transferred to smaller dimensions. However, with increasing miniaturization, so-called size effects take place [1], which inhibit sometimes the use of conventional manufacturing processes in total, or they can be used only with restrictions in micro range.

Typical components, where joining of thin foils play a role are, i.e. magnetic suspensions of hard-disc recorders [2], pressure sensor membranes and micro valves or micro motors [3]. At present for joining of thin sheets welding and brazing are used [4]. However, joining of non-matching materials leads to a dual character, where one joining partner melts, while the second stays in solid state. Joining of dissimilar materials can result in formation of diffusion-based intermetallic phases, which are characterized by high hardness and high brittle behavior. Furthermore, these processes lead to a thermal influenced material, what can be negative for the geometry of the components through distortion. In case of micro engineering these problems by thermal influences are particularly significant, since there is a high density of technical elements to be carried out next to heat sensitive components.

An accurate positioning of components is an important factor of joining micro engineering parts. Due to small dimension fixed components are difficult to access. Thus, non-contact processes have a high potential in micro engineering. Besides explosive-cladding additionally cladding joining process by forming, i.e. magnetic impact

welding, are on the rise [5]. The advantage of such processes is that they do not lead to typical heat affected zones or distortion and that the occurrence of intermetallic phases is minimized [6].

One approach for manufacturing thin metallic hybrid joints by non-contact impact joining was done by Nd:YAG-laser induced shock waves [7]. A thin foil (thickness ≤200 µm) was placed on a solid joining partner tilted by a process specific angle. For the protection of the surface and for increase of shock wave pressure an ablation layer was applied. Finally the foil is accelerated by laser induced shock wave in direction of the solid body. Due to surface roughness the joint was achieved. Thereby no intermetallic phases were observed and an increased micro hardness along the boundary layer after the joining could be measured [8].

Due to potential distortion at the possibility of joining different materials it can be summarized that for joining processes i.e. thermal processes like laser welding a limit is reached. Due to an ever rising demand of smallest sheet metal products and the named challenges it exists a strong need to develop new manufacturing processes. The main demands to join materials with different properties are a high accuracy, short process time and practicality. Thus, a new high speed joining process based on the laser shock forming process is developed, which enables a simple process handling and short process times without need of an ablation layer. Laser shock forming is a well known process, where laser shock treatment is extended to laser shock forming by a TEA-CO_2-laser. Due to laser treatment free electrons are generated by thermo emission out of the surface [9]. The number of free electrons depends on focus size, laser pulse intensity and surface material [9]. These free electrons absorb energy by inverse bremsstrahlung absorption and can produce further ions and electrons by impact processes until an optical breakdown and thus a plasma formation is achieved [10]. The inverse bremsstrahlung increases with the square of the wavelength accomplishing a nearly complete absorption of the longer wavelength of CO_2-laser light by the plasma. This kind of shock wave formation is known since the 70 s, e.g. [11]. If the energy density of the laser pulse exceeds a certain threshold, the fast expansion of the plasma forms a shock wave [12], which is initiated ∼5 mm above surface [11]. This shock wave moves spherically [13]. The pressure of the shock wave leads to a forming of the surface, e.g. [14]. During the laser shock forming process, pressure peaks in the range of some MPa can be achieved [15]. By a laser shock bending process with a maximum pulse energy of 5.5 J and a forming velocity of 40 m/s strain rates of 3×10^3 s^{-1} could be determined. By cone-shaped blank holder, which limits the spreading of the shock wave, the pressure can be increased [16]. The pressure wave has a

high tolerance against the focal position, therefore a correction of the focal position during a process with several pulses is not necessary [1]. Several pulses can be applied at the same position in order to achieve a high forming degree without increasing the energy density beyond ablation limit. Laser shock forming achieves higher strains than quasi-static forming methods [17].

The laser shock forming process can be used for deep drawing of copper and aluminum sheets, which was already presented in former publications [18]. Furthermore, laser shock forming enables manufacturing of undercuts in thin sheets [19], which are not possible by conventional forming methods. In this article these undercuts act as joint patch in the presented joining method by laser shock forming. One important factor for the quality of forming undercuts by laser shock forming is the pressure shock wave. Wielage and Vollertsen [20] showed that there is an influence of the decreasing pressure with growing distance from the shock wave ignition point for the quality of formation of the undercut. In order to specify this influence and make it useable for further studies in joining by laser shock forming, in this article the shock wave pressure distribution is measured. Due to the different environmental condition for the contact of the pressure wave with the material the investigations are done in open and closed environment. Furthermore, it is presented how joints by laser shock forming can be realized.

2 Experimental set-up

2.1 Joining process

For the joining process a pulsed TEA-CO_2-laser (wavelength: 10.6 µm) with a pulse duration of 100 ns, a spot are of 0.04 cm^2 and a laser pulse energy up to 6 J per pulse is used. The experimental setup for joining by laser shock forming is shown in Fig. 1. The setup consists out of five elements: the blank holder, the two joining partners, a spacer and the bottom of the tool. The two joining partners are positioned upon each other with a small overlap. The first joining partner includes a hole with a diameter of 4 mm for the material flow of the second joining partner. This hole is made by a laser cutting process and designates the geometry of the joint. As first joining partner stainless steel (1.4301) with a thickness of 100 µm and as second joining partner aluminum Al99.5 with a thickness of 50 µm is used. In order to enable material flow for the undercut formation there is a spacer between the two joining partners and the bottom. The height of the spacer can be changed. The blank holder is holding down the joining partners during the process with a blankholder force of 25 N. The laser irradiates on the first joining partner with
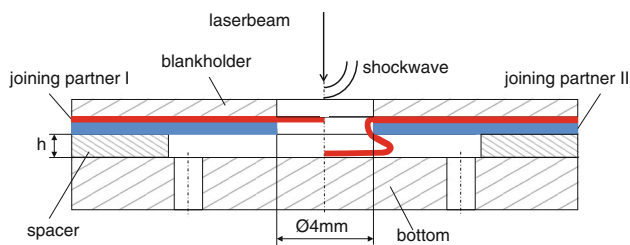
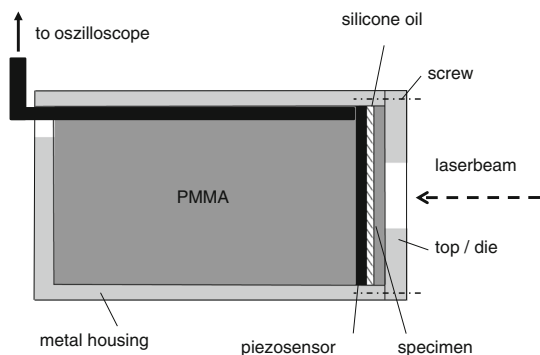**Fig. 1** Experimental setup for the joining process

Fig. 2 Plan of piezosensor measurement system

the focus on the surface and creates the plasma for the laser shockwave. This shockwave forms the material in the joining area and creates an undercut which presents the joint itself. For the experiment 50 pulses are used.

2.2 Pressure measurement method

The acting pressure of the plasma on the surface produces a shock wave at the solid body. The pressure caused by the laser induced shockwave is the basic physical parameter for the plastic forming of the work piece. For the evaluation of the laser shock joining method the pressure is measured in an open and in a tube environment by the following method.

In order to detect the pressure under the surface of the specimen a measurement system based on the work of Hintz [21] and Eisner [22] is used. For that a piezoelectric polyvinylidine fluoride (PVDF) sensor from Piezotech S.A.S. with an active area A of 1 mm^2 and total thickness of 75 µm, embedded in a PTFE foil, is bonded on the surface of a PMMA body, Fig. 2. This enables measuring without disadvantageous reflections of the initiated shockwave. After plasma ignition by laser the pressure wave starts spreading with 20,000 m/s [23] and thus it expands faster than the air can absorb it. Thus, an overload pressure is generated at the border of the plasma zone, which can only be stepwise emitted to the air, based on the high amplitude. High amplitudes λ are emitted by small frequencies f, since $\lambda \sim 1/f$ [24]. The response rate of the

piezosensor is up to 10^{-9} Hz hence it is suitable for shockwave measurement. For a better coupling of the shockwave into the sensor, silicone oil is placed between sensor and sample. The PMMA body is hold in a metal box, which consists of a metal housing with a top to eliminate high frequency interferences. The top is fixed by screws, which are tightened with defined torque of 10 N cm each. The sensor signal is read by a digital storage oscilloscope (Typ Waverunner-2 DSO) from LeCroy Corporation with an input impedance of 1 MΩ (input capacity 20 pF).

The introduced measurement setup provides the signal of the piezosensor as function of voltage over time. In order to determine the acting pressure p_p the acting force F per area at the sensor surface A_{Sensor} is determined:

$$p_P(t) = \frac{F}{A_{Sensor}} \tag{1}$$

The force acting on the sensor initiates a charge displacement $Q(t)$, which is proportional to the applied force F. Thereby the proportionality factor equates the piezoelectric constant d_{33} (field and deflection in direction of polarization) [25]:

$$Q(t) = d_{33} \cdot F \tag{2}$$

Charges cannot be measured directly. They are transferred in a voltage U_P by total capacity C_G [25]:

$$Q(t) = C_g \cdot U_P(t) \tag{3}$$

The used piezosensor consists out of 2 PVDF-layers, which are connected in parallel. The total capacity C_G of the sensor is given by the sum of the single capacities C_1 and C_2 of the 2 PVDF-layers. Since both layers have the same properties, C_G is 2 times C_1.

The total capacity C_G is than given by the electric field constant ε_0, the permittivity ε_r, the area of the plate capacitor (in this case the area of the sensor) A_{sensor} and distance between the plates d_P (in this case the distance between the two sensor strips) [25]:

$$C_g = \frac{2 \cdot \varepsilon_0 \cdot \varepsilon_r \cdot A_{Sensor}}{d_P} \tag{4}$$

By inserting (2), (3) and (4) in (1) the acting pressure p_p is:

$$p_P(t) = \frac{2 \cdot U_P(t) \cdot \varepsilon_0 \cdot \varepsilon_r}{d_P \cdot d_{33}} \tag{5}$$

With $\varepsilon_0 = 8.854 \times 10^{-12}$ As/Vm [24], ε_r (piezoeletric PVDF) = 12 [26], $d_P = 5$ µm (determined by cross section) and $d_{33} = 22.5$ pC/N (manufacture data) it is:

$$p_P(t) = 1.9 \cdot \frac{MPa}{V} \cdot U_P(t) \tag{6}$$

The pressure p_p measured by the piezosensor is lower than

286

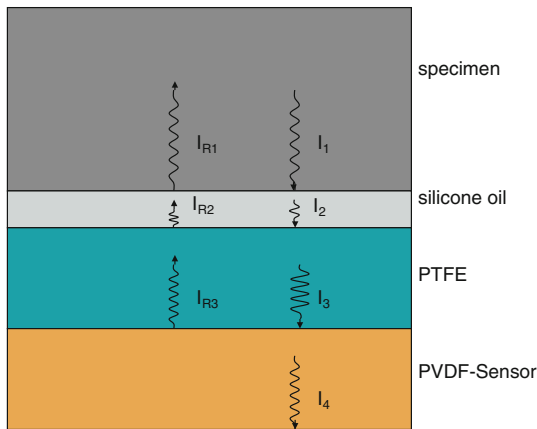Prod. Eng. Res. Devel. (2014) 8:283–290

Fig. 3 Different existing layers in the measurement system

the one on the specimen, since a part of the intensity of the pressure wave gets lost as reflections at the interfaces from specimen to silicone oil and from silicon oil to piezosensor. This loss can be determined by the acoustic impedances. The acoustic impedance Z is determined by the density ρ of a material and the phase velocity c of a wave in this medium:

$$Z = \rho \cdot c \tag{7}$$

By assuming a vertical incidence of the pressure wave for the intensity I_B at the interface between medium A and medium B it is [27]:

$$I_B = I_A \cdot \frac{4 \cdot Z_A \cdot Z_B}{(Z_A + Z_B)^2} \tag{8}$$

Figure 3 shows the different existing layers in the measurement system. The interfaces reflect a part of the intensity of the shock wave (I_{R1}, I_{R2}, I_{R3}). Thus, a correction factor Z_F is calculated out of the acoustic impedances of the four materials [see (7) and Table 1]:

$$\begin{aligned} Z_F &= \frac{I_1}{I_4} \\ &= \frac{(Z_{specimen} + Z_{Oil})^2}{4 \cdot Z_{specimen} \cdot Z_{Oil}} \cdot \frac{(Z_{Oil} + Z_{PTFE})^2}{4 \cdot Z_{Oil} \cdot Z_{PTFE}} \\ &\quad \cdot \frac{(Z_{PTFE} + Z_{PVDF})^2}{4 \cdot Z_{PTFE} \cdot Z_{PVDF}} \end{aligned} \tag{9}$$

Due to calibration data of the piezosensor, the real pressure p_s under the specimen it is:
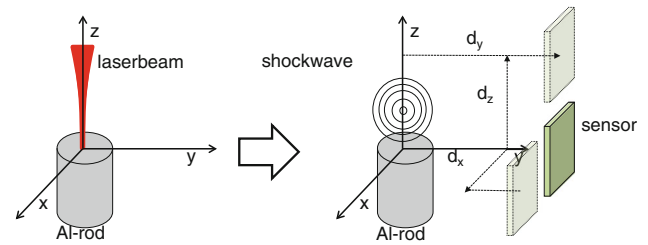
$$p_s(t) = Z_F \cdot p_p(t) \tag{10}$$

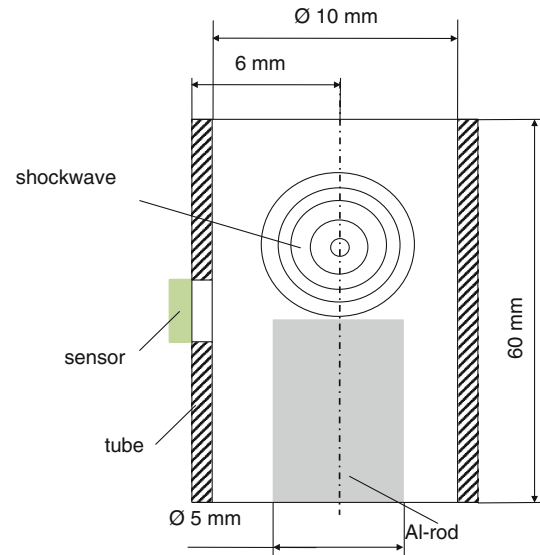**Fig. 4** Experimental set-up for the pressure measurement in open environment

Fig. 5 Experimental setup for measuring the pressure distribution in a closed environment

Thus, the acting pressure p_s over time t can be determined. For the following investigations the maximum pressure p_{max} of acting pressure over time curve is determined.

2.3 Pressure measurement conditions

In order to get knowledge about the shockwave pressure distribution in open and closed environment the described pressure measurement system is positioned at different distances in x-, y- and z-direction from the specimen surface. As external ignition specimen an aluminum rod with a diameter of 5 mm is used. The focus of the laser is in the center of the facing surface of the rod. This point is defined as the origin of the coordinate system for the test setup. Every change in the position of the sensor will be made in

Table 1 Acoustic impedances of different materials (data from [27–29]) and the calculated correction factor Z_F for aluminum

Specimen material	$Z_{specimen}$	Z_{Oil}	Z_{PTFE}	Z_{PVDF}	Z_F
Aluminum	17×10^6 kg/(m² s)	1.35×10^6 kg/(m² s)	2.97×10^6 kg/(m² s)	3.9×10^6 kg/(m² s)	4.3
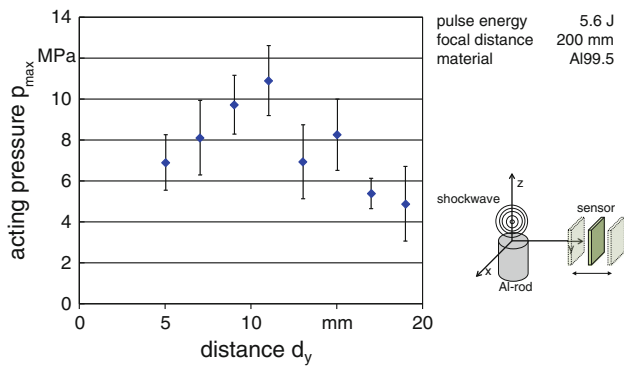
Fig. 6 Pressure distribution of the shockwave in y-direction

Fig. 7 Pressure distribution of the shockwave in z-direction

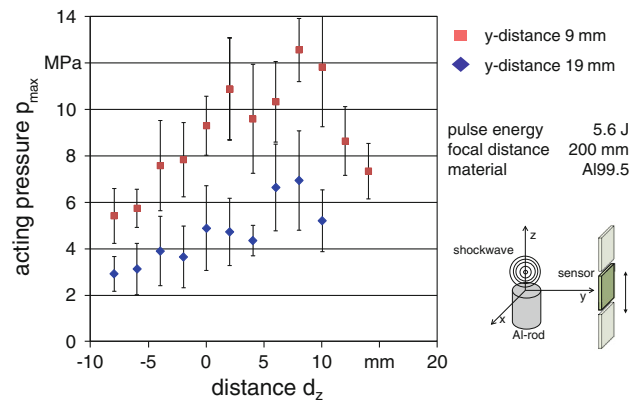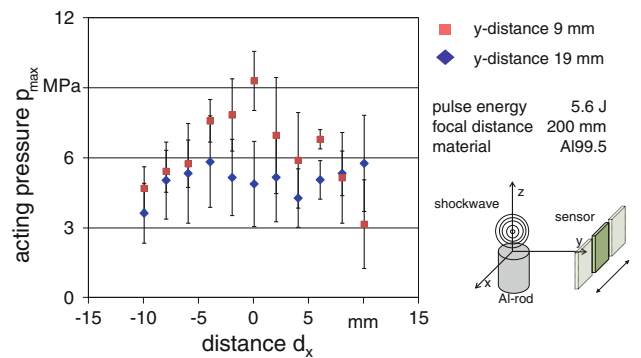Fig. 8 Pressure distribution of the shockwave in x-direction

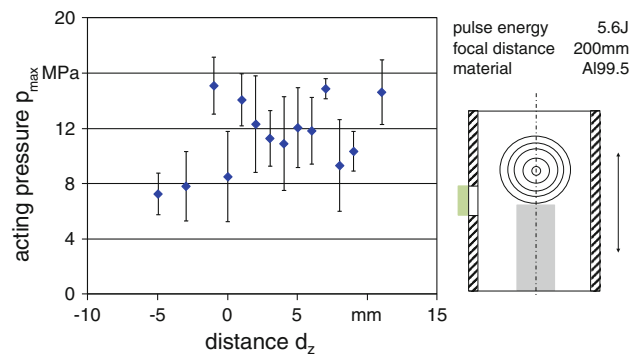Fig. 9 Pressure of the shockwave inside a tube in different z-positions

relation to this coordinate system. Figure 4 shows the position of the coordinate system and the sensor system.

The experimental setup for measuring the pressure distribution in a closed environment is shown in Fig. 5. Therefore, the sensor is mounted to a tube out of Al99.5 with an inner diameter of 10 mm and a length of 60 mm. This configuration ensures that the plasma ignites inside the tube. For each position 6 measurements were made. After 50 measurements the surface of the aluminum rod is refurbished by removing 1 mm from the surface by a turning process. This ensures that the surface of the aluminum rod is not changing significantly between the measurements.

3 Results

3.1 Acting pressure distribution

In order to measure the shockwave pressure distribution in open environment the maximum acting pressure p_{max} is determined in different distances in x-, y- and z-direction to the aluminum rod, which is used for plasma ignition. Results of the measurement in y-direction are shown in Fig. 6. Due to the experimental setup it is not possible to go closer to the center than 5 mm. It is visible that the pressure increases linear with the distance to the center of the rod. The highest pressure of about 11 MPa is achieved at a distance of $d_y = 11$ mm to the center of the coordinate system.

Figure 7 shows the results of the acting pressures in different z-positions. In order to get an idea of pressure distribution the pressures in z-direction are measured in y-axis positions d_y of 9 and 19 mm. All other parameter kept constant. The results in Fig. 7 show that the acting pressures in a distance d_y of 19 mm of the rod center increase up to 8 mm displacement in positive direction, where the biggest value of about 7 MPa is reached. For a displacement of more than 8 mm the pressures decrease.

Furthermore, it can be seen that with increasing pressure the standard deviation is increasing, too. The pressures measured in closer position to the rod center ($d_y = 9$ mm) show a constant behavior in z-direction between $d_z = 3$ mm and $d_z = 10$ mm and achieve acting pressures of about 12 MPa.

The measurements of the pressures in x-direction are made in a y-distance d_y of 19 mm. The results in Fig. 8 show that the pressure of some 5 MPa is not significantly dependent on the x-position. The standard deviation is high

288

Prod. Eng. Res. Devel. (2014) 8:283–290

compared to the measured values, what is based on the measurement system and plasma ignition process. For each configuration six measurements were performed.

In order to determine the pressure distribution in closed environment, it is measured in the tube at different z-axis position. Figure 9 shows the results. It is visible that a wide range the values are nearly constant with about 12–14 MPa. Only at a displacement of $d_y = -4$ mm of the sensor the pressure drops to 8 MPa.

3.2 Acting pressure/time-characteristic

In order to get a closer view on the acting pressure behavior over time, the characteristic is exemplary displayed in Fig. 10 in open environment compared to the pressure in the tube. The characteristic curves are recorded for a z-position of $d_z = 6$ mm. The y-distance of the sensor is 6 mm for the tube environment and 9 mm for the open environment. It is visible that the pressure in the tube shows several periodical pressure maxima.
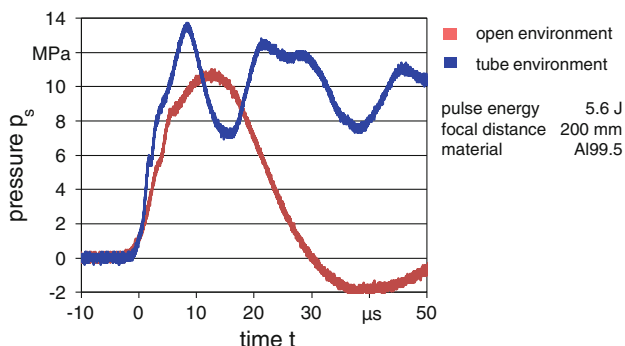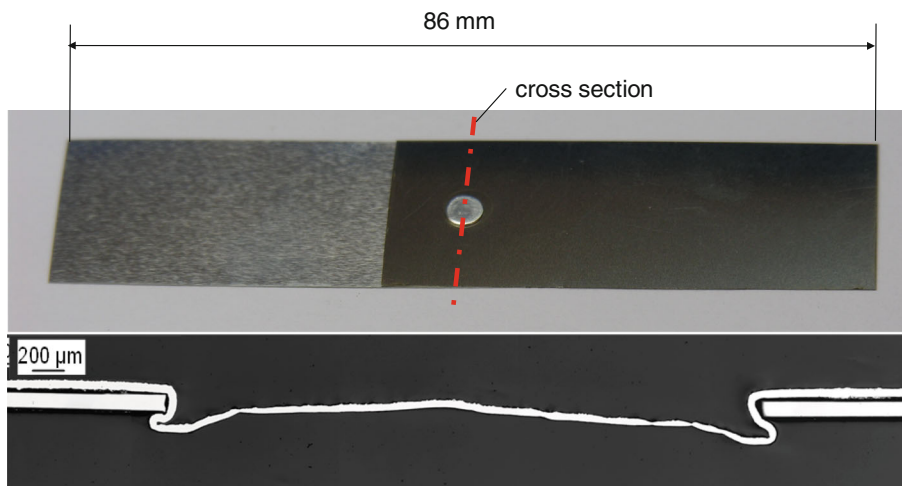

Fig. 10 Characteristic of acting pressure versus time

Fig. 11 Joint and cross section of a joint, diameter of the die: 4 mm, pulse energy: 5.6 J, number of pulses: 50, material: 1.4301(material thickness: 100 μm)/Al99.5 (material thickness: 50 μm)

3.3 Realization of the joint

With the experimental setup described above it is possible to create a joint. According to the experimental setup the laser irradiates on the surface of joining partner I, so that the joining specimen is also used as ignition specimen. Figure 11 shows a joint produced by laser induced shockwaves and a cross section of a joining. The cross section was made along the red line. It can be seen, that the aluminum foil is creating an undercut behind the steel sheet. The bottom of the aluminum undercut shows a buckling.

4 Discussion

In this article the maximum acting pressure distribution was measured in open and closed environment. It is shown for the results for an open environment with a displacement of the sensor in z-direction, that the maximum pressure is measured about 8 mm above the surface of the aluminum rod. This value is achieved at a sensor distance of 19 mm to the center of the rod. However, the results achieved in the test series at a distance of 19 mm are consistent with the studies of Barchukov et al. [11]. They suggested that a laser induced plasma is detonating about 5 mm above the surface on which the laser irradiates. This one rough value is stated for their experiments, which were done with a CO_2-laser and different material like aluminum, copper and magnesium. Thus, from the present investigations in this article it can be more precisely stated, that for a plasma ignition out of aluminum treated by a TEA-CO_2-laser the point of ignition is about 8 mm above the surface.

According to Fig. 6 the pressure values increase up to 11 mm and decrease to smaller distances than 11 mm. This can be explained by the geometry of the measurement device and the point of ignition above the surface. Due to
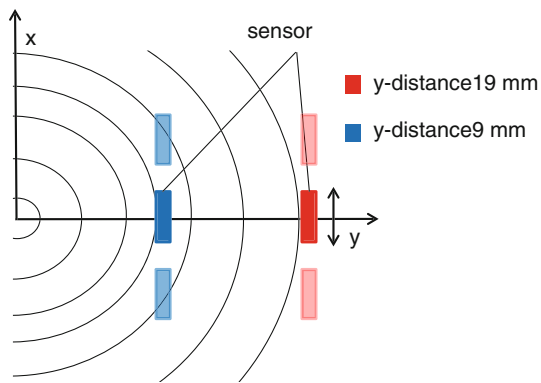
Prod. Eng. Res. Devel. (2014) 8:283–290

289

Fig. 12 Sensor position and shock wave propagation

the die which fixes the specimen in the pressure measurement setup the shockwave cannot hit the sample directly, because it produces a shadowing effect. This leads to a decrease of the pressure values and explains the effect shown in Fig. 6.

The pressure distribution in x-direction shows a different behavior. Between $d_x = -10$ mm and $d_x = 10$ mm the pressure keeps nearly constant at about 5 MPa for the sensor distance of 19 mm, Fig. 8. For the results at a sensor distance of $d_y = 9$ mm the pressure values decrease with increasing deviation from the center. Here one effect of the spherical propagating shock wave carries weight, displayed in Fig. 12: Since the laser induced shockwave is propagating as a sphere, the angle of impact is more different at different z-positions at closer distance. With higher distance to the center of the plasma a smooth distribution of the shockwave takes place, so that at higher distances the influence of a displacement decreases.

For the results with the experimental tube setup it can be seen that the acting pressure is alternating around 12 MPa over the displacement of the sensor in positive direction. One reason for this can be found in the pressure–time characteristics, Fig. 10. In comparison to a pressure–time characteristic in open environment, the characteristics from the pressure measurement in the tube show several periodical pressure maxima. This can be explained by multiple reflections at the wall of the tube and compression in the tube.

Furthermore, it could be shown, that joints out of two thin sheets can be realized by laser shock forming. Nevertheless, Fig. 11 shows a buckling of the formed part at the bottom. This can be explained by backstroke effect. In further investigations this can be minimized by an intake through a ventilation fitting [30] and regulated by the knowledge of the pressure distribution, which was determined in this article.

Summarized it can be said, that the position of the plasma ignition is about 8 mm above the surface. This information is important for the use of the shockwave in near field applications, where high pressure values are needed. For a far field use of the shockwave it can be said, that due to the pressure distribution at higher distances to the center of the shockwave, an exact position plays a minor role in the process. This leads to a stable manufacturing process. Referred to the pressure distribution in a tube environment, where a nearly constant pressure distribution with high pressure values can be achieved, a process which is almost independent from the position is presented.

5 Conclusion

- Joining of thin sheets in micro range is possible by laser induced shock waves.
- The ignition point of the TEA-CO$_2$-laser induced plasma out of aluminum is about 8 mm above the surface.
- Nearly location independent high acting pressures can be realized in a tube.

References

1. Vollertsen F, Biermann D, Hansen HN, Jawahir IS, Kuzman K (2009) Size effects in manufacturing of metallic components. CIRP Ann Manuf Technol 58(2):566–587
2. Sam R, Yu B, Chen M, Eagleson M (2001) Advances in laser microwelding. In: Chen X (ed) Proceedings of 20th international congress on applications of lasers and electro-optics (ICALEO 2001). 15–18 Oct 2001, Jacksonville, FL, USA, F402
3. Kamada K, Nakamura Y, Ohmori A, Matsunawa A, Katayama S, Arata Y (1987) Application of laser welding to production of micro-motor coil. In: Proceedings of international conference on laser advanced materials processing (LAMP '87). May 21–23 1987, Osaka, Japan, pp 573–578
4. Smolka G, Gillner A, Bosse L, Lützeler R (2004) Micro electron beam welding and laser machining—potentials of beam welding methods in the micro-system technology. Microsyst Technol 10:187–192
5. Neugebauer R, Bouzakis K-D, Denkena B, Klocke F, Sterzing A, Tekkaya AE, Wertheim R (2011) Velocity effects in metal forming and machining processes. CIRP Ann Manuf Technol 60(2):627–650
6. Zhang Y, Babu S, Daehn GS (2010) Impact welding in a variety of geometric configurations. In: 4th international conference on high speed forming, pp 97–107
7. Patent (USA) (2011) Low-temperature spot impact welding driven without contact. Pub. No. US 2011/0000953 A1
8. Zhang Y, Suresh Babu S, Prothe C, Blakely M, Kwasegroch J, LaHa M, Daehn GS (2011) Application of high velocity impact welding at varied different length scales. J Mater Process Technol 211:944–952

9. Demtröder W (2010) Atoms, molecules and photons an introduction to atomic-, molecular-, and quantum-physics, 2nd edn. Springer, Berlin, p 37

10. Miziolek AW, Palleschi V, Schechter I (2006) Laser induced breakdown spectroscopy, 1st edn. Cambridge University Press, Cambridge

11. Barchukov AI, Bunkin FV, Konov VI, Lyubin AA (1974) Investigation of low-threshold gas breakdown near solid targets by CO_2 laser radiation. Sov Phys-JETP 39–3:469–477

12. O'Keefe JD, Skeen CH, York CM (1973) Laser-induced deformation modes in thin metal targets. J Appl Phys 44(10):4622–4626

13. Walter D, Michalowski A, Gauch R, Dausinger F (2007) Monitoring of the micro-drilling process by means of laser-induced shock waves. In: Vollertsen F, Emmelmann C, Schmidt M, Otto A (eds) Proceedings of the fourth international WLT-conference on lasers in manufacturing (LIM07). AT-Fachverlag, Stuttgart, pp 557–562

14. Zhang W, Yao YL, Noyan IC (2004) Microscale laser shock peening of thin films, part 1: experiment, modeling and simulation. ASME 126:10–17

15. Vollertsen F, Schulze Niehoff H, Wielage H (2009) On the acting pressure in laser deep drawing. Prod Eng Res Dev 3(1):1–8

16. Wielage H, Vollertsen F (2010) Increase of acting pressure by adjusted tool geometry in laser shock forming. In: Chinesta F, Chastel Y, El Mansori M (eds) Proceedings of international conference on advances in materials and processing technologies (AMPT2010). Paris (France), 24–27 Oct 2010, AIP Conference Proceedings, Melville, New York, pp 763–768

17. Vollertsen F, Blaurock L (2009) Einfluss der Umformgeschwindigkeit und der Messauflösung auf das Formänderungsverhalten in der Mikroblechumformung. In: Vollertsen F, Büttgenbach S, Kraft O, Michaeli W (eds) 4th kolloquium mikroproduktion. BIAS-Verlag, Bremen, pp 243–252

18. Wielage H, Schulze Niehoff H, Vollertsen F (2008) Forming behavior in laser shock deep drawing. In: International conference on high speed forming 2008, ICHSF 2008, Proceedings. University of Dortmund, Institut für Umformtechnik und Leichtbau, Dortmund, Germany, March 11–12 2008, pp 213–222

19. Wielage H, Vollertsen F (2011) Undercuts by laser shock forming. In: The 14th international ESAFORM conference on material forming. AIP conference proceedings 1353. American Institute of Physics, ISBN 978-0-7354-0911-8, pp 1309–1312

20. Wielage H, Vollertsen F (2011) Analysis of fracture behavior in plastic shaping by laser shock forming. In: Proceedings international conference on technology of plasticity (ICTP) 2011, 25–30 Sept 2011, Aachen, Deutschland, pp 1076–1080

21. Hintz G (1997) Untersuchung der Druckerzeugung und der Strahl-Stoff-Wechselwirkung an einem Excimerlaser-System für die Schockbehandlung von Metallen. Dissertation, Universität Erlangen-Nürnberg

22. Eisner K (1998) Prozeßtechnologische Grundlagen zur Schockverfestigung von metallischen Werkstoffen mit einem kommerziellen Excimerlaser. Dissertation, Universität Erlangen-Nürnberg

23. Li Q, Hong Y, Ye J, Wen M, Wang G (2010) Study of the velocity of a laser supported detonation wave, lasers in engineering, vol 19. Old City Publishing, Philadelphia, pp 153–161

24. Träger F (2012) Springer handbook of lasers and optics. Springer, Berlin, p 95

25. Fraden J (2010) Handbook of modern sensors: physics, designs, and applications, 4th edn. Springer, Berlin, p 86ff

26. Sulemann A (2001) Smart structures: applications and related technologies (CISM international centre for mechanical sciences). Springer, Berlin, p 5

27. Sanches JM, Laine AF, Suri JS (2012) Ultrasound imaging: advances and applications. Springer, Berlin, p 286f

28. Shull PJ (2002) Nondestructive evaluation: theory, techniques, and applications (Dekker mechanical engineering), 1st edn. CRC Press, Boca Raton, FL, p 91

29. Wüstenberg H, Rotter B, Erhard A, Möhrle W, Pitkänen J (1989) A parametric study of ultrasonic probes with PVDF-Transducers. In: Boogard J, van Dijk GM (eds) Proceedings 12th world conference on non-destructive testing. Elsevier, Amsterdam, NL, pp 691–698

30. Wielage H, Vollertsen F (2012) Difficulties and prevention methods in mechanical and non-mechanical micro drawing with high work piece velocities. In: Yuan SJ, Vollertsen F, Wang ZR, Dean TA (eds) Proceedings of the 3rd international conference on new forming technology (INCFT), Harbin, China, Aug 26–28, 2012, China, pp 24–29